# LETTER

Long-term decline of the Amazon carbon sink

A list of authors and their affiliations appears at the end of the paper

Atmospheric carbon dioxide records indicate that the land surface has acted as a strong global carbon sink over recent decades[1,2], with a substantial fraction of this sink probably located in the tropics[3], particularly in the Amazon[4]. Nevertheless, it is unclear how the terrestrial carbon sink will evolve as climate and atmospheric composition continue to change. Here we analyse the historical evolution of the biomass dynamics of the Amazon rainforest over three decades using a distributed network of 321 plots. While this analysis confirms that Amazon forests have acted as a long-term net biomass sink, we find a long-term decreasing trend of carbon accumulation. Rates of net increase in above-ground biomass declined by one-third during the past decade compared to the 1990s. This is a consequence of growth rate increases levelling off recently, while biomass mortality persistently increased throughout, leading to a shortening of carbon residence times. Potential drivers for the mortality increase include greater climate variability, and feedbacks of faster growth on mortality, resulting in shortened tree longevity[5]. The observed decline of the Amazon sink diverges markedly from the recent increase in terrestrial carbon uptake at the global scale[1,2], and is contrary to expectations based on models[6].

The response of the Earth's land surface to increasing levels of atmospheric CO_2 and a changing climate provide important feedbacks on future greenhouse warming[6,7]. One of the largest ecosystem carbon pools on Earth is the Amazon forest, storing around 150–200 Pg C in living biomass and soils[8]. Earlier studies based on forest inventories in the Amazon Basin showed the tropical forest here to be acting as a strong carbon sink with an estimated annual uptake of 0.42–0.65 Pg C yr^{-1} for 1990–2007, around 25% of the residual terrestrial carbon sink[3,4]. There is, however, substantial uncertainty as to how the Amazon forest will respond to future climatic and atmospheric composition changes. Some earlier modelling studies predicted a large-scale dieback of the Amazon rainforest[9], while more recent studies predict a carbon sink well into the twenty-first century due to a CO_2 fertilization effect[6]. The realism of such model predictions remains low owing to uncertainty associated with future climate and vegetation responses[6,7] in particular changes in forest dynamics[5,10,11]. Thus, direct observations of tropical tree responses are crucial to examine what changes are actually occurring and what to expect in the future. Here we analyse the longest and largest spatially distributed time series of forest dynamics for tropical South America.
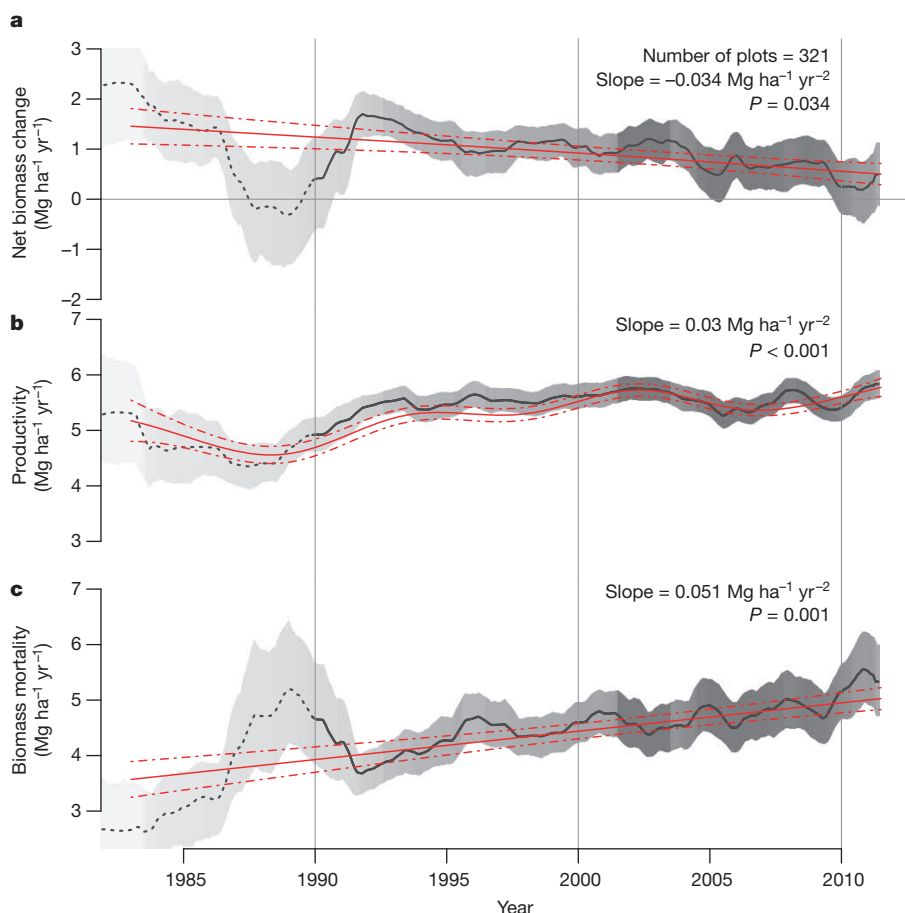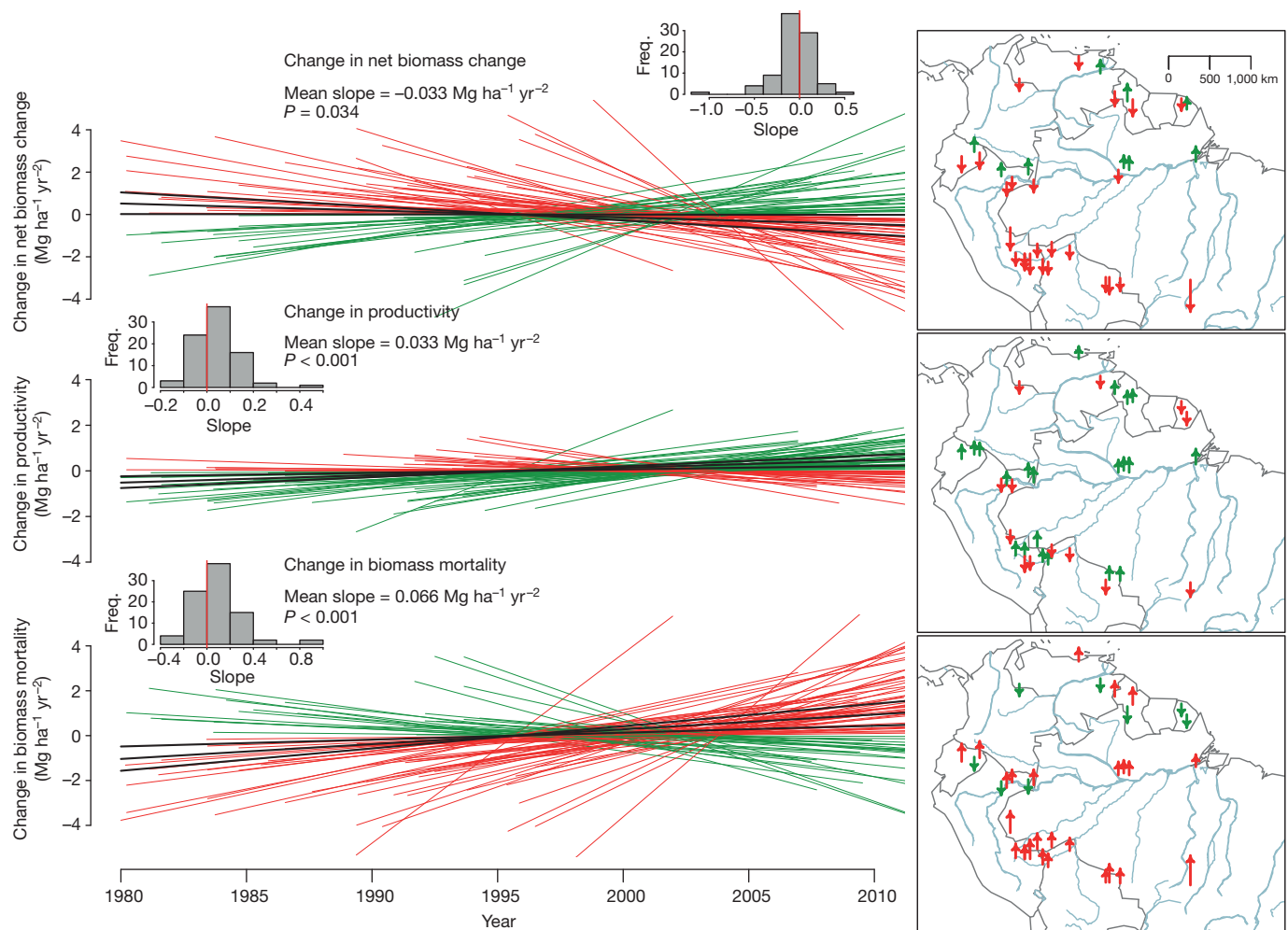

Figure 1 | Trends in net above-ground biomass change, productivity and mortality across all sites. a–c, Black lines show the overall mean change up to 2011 for 321 plots (or 274 units) weighted by plot size, and its bootstrapped confidence interval (shaded area). The red lines indicate the best model fit for the long-term trends since 1983 using general additive mixed models (GAMM), accounting explicitly for differences in dynamics between plots (red lines denote overall mean, broken lines denote s.e.m.). Alternative analyses of subsets of plots that were all continuously monitored throughout shorter time intervals confirm that the observed trends are not driven by temporal changes in individual sample plot contributions (Extended Data Fig. 3). Estimated long-term (linear) mean slopes and significance levels are indicated, and are robust with regard to the statistical approach applied (that is, parametric or non-parametric, see Methods). Shading corresponds to the number of plots that are included in the calculation of the mean, varying from 25 plots in 1983 (light grey) to a maximum of 204 plots in 2003 (dark grey). The uncertainty and variation is greater in the early part of the record owing to relatively low sample size (see Extended Data Fig. 4).

In figure panel a:
Number of plots = 321
Slope = −0.034 Mg ha^{-1} yr^{-2}
$P = 0.034$

In figure panel b:
Slope = 0.03 Mg ha^{-1} yr^{-2}
$P < 0.001$

In figure panel c:
Slope = 0.051 Mg ha^{-1} yr^{-2}
$P = 0.001$

Our analysis is based on 321 inventory plots lacking signs of recent anthropogenic impacts from the RAINFOR network[4] and published plots. The sites are distributed throughout the Amazon basin and cover all major forest types, soils and climates (Extended Data Fig. 1). For each plot (mean size 1.2 ha) all trees with stem diameter greater than 100 mm were identified, and allometric equations applied to convert tree diameter, height and wood density to woody biomass or carbon[8]. Net biomass change was estimated for each census interval as the difference between standing biomass at the end and the beginning of the interval divided by the census length. We also derived forest woody productivity (hereafter termed productivity) from the sum of biomass growth of surviving trees and trees that recruited (that is, reached a diameter ≥ 100 mm), and mortality from the biomass of trees that died between censuses, allowing for census-interval effects (see Methods). Plots were measured on average five times and the mean measurement period was 3 years. For analysis purposes small plots were aggregated to leave 274 distinct units. We report trends since 1983, the first year with measurements for 25 plots, up to mid-2011.

Our data show that mature forests continued to act as a biomass sink from 1983 to 2011.5, but also reveal a long-term decline in the net rate of biomass increase throughout the census period (Fig. 1a). The decline

in net biomass change is due to a strong long-term increase in mortality rates (Fig. 1c), and occurred despite a long-term increase in productivity (Fig. 1b). While mortality increased throughout the period, productivity increases have recently stalled showing no significant trend since 2000 (Extended Data Fig. 3). These time trends are based on a varying set of plots over time (Extended Data Fig. 4), but this site-switching does not alter the results (see Methods). The observed trends also emerge from a separate plot-by-plot analysis (Fig. 2), with increases in mortality exceeding productivity gains by approximately two to one. Trends are rarely significant at the individual plot level owing to the stochastic nature of local forest dynamics, but the mean slopes of net change, productivity and mortality all differ significantly from zero. Changes in forest dynamics were not geographically limited to a particular area, but occurred throughout the lowland South American tropics (Fig. 2). While rates of change vary depending on the precise plot set, time window and analytical approach used, the trends remain robust (Figs 1, 2 and Extended Data Fig. 3).

Artefactual explanations have previously been offered to explain trends in biomass dynamics from plot measurements[12,13]. Principally, it has been suggested that reported net biomass increases[4] could be driven by recovery of forests from local disturbances[12]. However, contrary to

Figure 2 | Annual change in net above-ground biomass change, productivity and mortality for individual sites. The lines in the left-hand panels show the long-term rate of change for 117 plots (or 87 units), estimated using linear regressions weighted by census-interval length and for display purposes centred around zero. This analysis includes only plots that were monitored for at least 10 years and contained three or more census intervals with at least one in the 1990s and one in 2000s. Red lines indicate long-term trends that negatively affect biomass stocks (for example, decreasing net

change, increasing losses) and green lines indicate trends that positively affect biomass stocks (for example, increasing productivity). Bold black lines indicate the mean slope across all plots and confidence intervals (2.5–97.5 percentiles). Insets in the left panels show the frequency distribution of the slopes, with the mean slope and P value for t-test of difference from no slope. The maps show the location of the sites, and the colour and arrow length indicate the sign and magnitude of the slope, with adjacent plots joined into a single site for display purposes.

observations from recovering neotropical forests[14] and successional studies[15], the plots have collectively experienced increased biomass growth (Fig. 1), accelerated stem recruitment and death (Extended Data Fig. 6), and net biomass change is positively related to changes in stem numbers, but not in wood density (Fig. 3b, c). It is thus unlikely that the overall patterns would be driven by recovery from disturbances. Alternatively, increases in mortality have been proposed to arise due to biased selection of plots in mature forest patches, which over time accumulate disturbances and so decline in biomass[13]. The fact that forests and trees have continued to get bigger (Extended Data Fig. 5a) is contrary to this explanation. In addition, if this were driving the network-wide pattern, then the observed trends should disappear if data are reanalysed using only the first interval of each plot, but instead they persist. In summary, the data suggest that trends are unlikely to be caused by artefactual explanations of forests recovering from disturbances or selection of mature forest patches (see Supplementary Information for a more complete exploration of these potential biases).

The factors driving the observed long-term changes remain unclear. The levelling off of productivity in the most recent decade (Fig. 1b and Extended Data Fig. 3f) could be due either to a relaxation of the growth stimulus itself, or to the onset of a counteracting factor depressing growth rates. The recent demonstration of Amazon-wide carbon sink suppression during a drought year[16] indicates one possible driver. Tropical drought is also often associated with higher temperatures, which may further contribute to reducing productivity[17] and carbon uptake[18]. The past decade in Amazonia has seen several droughts[19] and warming[20], which coincide closely with the stalling productivity across Amazon forests.

The increased rate of biomass mortality is driven by an increasing number of trees dying per year (Extended Data Fig. 6c) rather than an increase in the size of the dying trees (Extended Data Fig. 5c). Several mechanisms may explain this increase in loss of biomass due to tree mortality, with recent climate events being an obvious candidate. The plot data clearly show short-term peaks in the size of dying trees during the anomalously dry years 2005 and 2010 (Extended Data Fig. 5c). These are consistent with results from rainfall exclusion experiments in Amazonia[21,22] and observations[4] showing that large tropical trees are vulnerable to drought stress. However, our data lack the signature expected if drought were the dominant long-term driver of the increasing loss of biomass due to mortality in Amazonia. That is, there has been no long-term change in the size of dead trees (Extended Data Fig. 5c), living trees have continued to get bigger (Extended Data Fig. 5a), and the increase in stem mortality predates the drought of 2005 (Extended Data Fig. 6c).

Alternatively, the increased productivity may have accelerated tree life cycles so that they now die younger. Large stature is associated with size-related hydraulic[23] and mechanical failure[24], reproductive costs[25] and photosynthetic decline[23]. Faster growth exposes trees to these size-related risks earlier, as evidenced by tree ring data suggesting that faster growth shortens lifespans[26,27], and by experimental data showing early onset of reproduction under increased CO_2 (ref. 28). The observed long-term acceleration in stem mortality rates and the plot-level association between productivity and the strength of the increase in biomass loss due to mortality (Extended Data Fig. 8b) are consistent with such a mechanism. While demographic feedbacks are not explicitly included in dynamic global vegetation models[10], our results suggest that they could in fact influence the capacity of forests to gain biomass[29], with transient rates of ecosystem net carbon accumulation highly sensitive to even small changes in carbon turnover times[10].

Finally, we put our results in a global perspective. According to global records, the land carbon sink has increased since the mid-1990s (refs 1, 2). While tropical land contributed significantly to this global sink during the 1980s and 1990s, our results show that the total net carbon sink into intact Amazon live biomass then decreased by 30% from 0.54 Pg C yr^{-1} (confidence interval 0.45–0.63) in the 1990s to 0.38 Pg C yr^{-1} (0.28–0.49) in the 2000s (see Methods). If our findings for the Amazon are representative for other tropical forests, and if below-ground pools have responded in the same way as above-ground biomass (AGB), then an apparent divergence emerges between a strengthening global terrestrial sink on one hand[1,2] and a weakening tropical sink on the other. However, from an atmospheric perspective we also note that some of the effects of the Amazon changes are yet to be observed, as little of the carbon resulting from increased mortality is immediately released into the atmosphere[30]. Instead, dead trees decay slowly, with a fraction also moving into a long-term soil carbon pool. The Amazon forest sink has therefore become increasingly skewed towards gains in the necromass pools, inducing a substantial lag in the probable atmospheric response. On the basis of the observed long-term increase in mortality rates, we estimate that the atmosphere has yet to see ~3.8 Pg of the Amazon necromass carbon produced since 1983 (see Methods), representing a 30% increase in necromass stocks. The modelled increase in Amazon necromass is twice the magnitude of the cumulative decadal decline in the live biomass sink from the 1990s to the 2000s (from 5.4 to 3.8 Pg C).

In summary, we find that the Amazon biomass carbon sink has started to decline, due to recent levelling of productivity increases, combined with a sustained long-term increase in tree mortality. This behaviour is at odds with expectations from models of a continually strong tropical
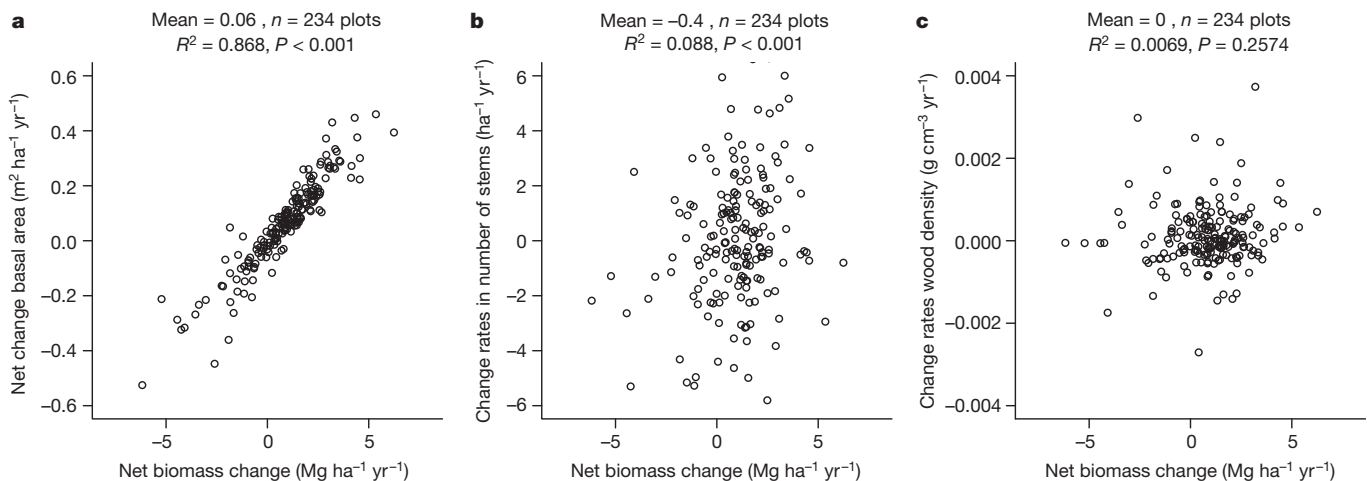
Figure 3 | Relationships between annual net change in biomass of individual plots and their annual change in basal area, stem numbers and wood density. a–c, The mean values of the rates of changes for basal area (**a**), stem numbers per hectare (**b**) and wood density (**c**) are given in each panel along with the R^2 of the relationship with annual net biomass change and the P value of the linear relationship. The number of plots included is 234 (that is, those with data on change in basal area, stem numbers and wood density).

biomass sink[6], and underlines how difficult it remains to predict the role of land-vegetation feedbacks in modulating global climate change[7,10]. Investment in consistent, coordinated long-term monitoring on the ground is fundamental to determine the trajectory of the planet's most productive and diverse biome.

Online Content Methods, along with any additional Extended Data display items and Source Data, are available in the online version of the paper; references unique to these sections appear only in the online paper.

1. Ballantyne, A. P., Alden, C. B., Miller, J. B., Tans, P. P. & White, J. W. C. Increase in observed net carbon dioxide uptake by land and oceans during the past 50 years. *Nature* **488**, 70–72 (2012).
2. Le Quéré, C. *et al.* The global carbon budget 1959–2011. *Earth System Science Data* **5**, 165–185 (2013).
3. Pan, Y. *et al.* A large and persistent carbon sink in the world's forests. *Science* **333**, 988–993 (2011).
4. Phillips, O. L. *et al.* Drought sensitivity of the Amazon rainforest. *Science* **323**, 1344–1347 (2009).
5. Bugmann, H. & Bigler, C. Will the CO_2 fertilization effect in forests be offset by reduced tree longevity? *Oecologia* **165**, 533–544 (2011).
6. Huntingford, C. *et al.* Simulated resilience of tropical rainforests to CO_2-induced climate change. *Nature Geosci.* **6**, 268–273 (2013).
7. Booth, B. B. B. *et al.* High sensitivity of future global warming to land carbon cycle processes. *Environ. Res. Lett.* **7**, 024002 (2012).
8. Feldpausch, T. R. *et al.* Tree height integrated into pantropical forest biomass estimates. *Biogeosciences* **9**, 3381–3403 (2012).
9. Cox, P. M., Betts, R. A., Jones, C. D., Spall, S. A. & Totterdell, I. J. Acceleration of global warming due to carbon-cycle feedbacks in a coupled climate model. *Nature* **408**, 184–187 (2000).
10. Friend, A. D. *et al.* Carbon residence time dominates uncertainty in terrestrial vegetation responses to future climate and atmospheric CO2. *Proc. Natl Acad. Sci.* **111**, 3280–3285 (2013).
11. Phillips, O. L. & Gentry, A. H. Increasing turnover through time in tropical forests. *Science* **263**, 954–958 (1994).
12. Fisher, J. I., Hurtt, G. C., Thomas, R. Q. & Chambers, J. Q. Clustered disturbances lead to bias in large-scale estimates based on forest sample plots. *Ecol. Lett.* **11**, 554–563 (2008).
13. Condit, R. Forest turnover, diversity, and CO2. *Trends Ecol. Evol.* **12**, 249–250 (1997).
14. Chambers, J. Q. *et al.* Response of tree biomass and wood litter to disturbance in a Central Amazon forest. *Oecologia* **141**, 596–611 (2004).
15. van Breugel, M., Martínez-Ramos, M. & Bongers, F. Community dynamics during early secondary succession in Mexican tropical rain forests. *J. Trop. Ecol.* **22**, 663–674 (2006).
16. Gatti, L. V. *et al.* Drought sensitivity of Amazonian carbon balance revealed by atmospheric measurements. *Nature* **506**, 76–80 (2014).
17. Clark, D. A., Clark, D. B. & Oberbauer, S. F. Field-quantified responses of tropical rainforest aboveground productivity to increasing CO2 and climatic stress, 1997–2009. *J. Geophys. Res.* **118**, 783–794 (2013).
18. Wang, X. *et al.* A two-fold increase of carbon cycle sensitivity to tropical temperature variations. *Nature* **506**, 212–215 (2014).
19. Marengo, J. A., Tomasella, J., Alves, L. M., Soares, W. R. & Rodriguez, D. A. The drought of 2010 in the context of historical droughts in the Amazon region. *Geophys. Res. Lett.* **38**, L12703 (2011).
20. Jiménez-Muñoz, J. C., Sobrino, J. A., Mattar, C. & Malhi, Y. Spatial and temporal patterns of the recent warming of the Amazon forest. *J. Geophys. Res.* **118**, 5204–5215 (2013).
21. da Costa, A. C. L. *et al.* Effect of 7 yr of experimental drought on vegetation dynamics and biomass storage of an eastern Amazonian rainforest. *New Phytol.* **187**, 579–591 (2010).
22. Nepstad, D. C., Tohver, I. M., Ray, D., Moutinho, P. & Cardinot, G. Mortality of large trees and lianas following experimental drought in an Amazon forest. *Ecology* **88**, 2259–2269 (2007).
23. Ryan, M. G., Phillips, N. & Bond, B. J. The hydraulic limitation hypothesis revisited. *Plant Cell Environ.* **29**, 367–381 (2006).
24. Lieberman, D., Lieberman, M., Peralta, R. & Hartshorn, G. S. Mortality patterns and stand turnover rates in a wet tropical forest in Costa Rica. *J. Ecol.* **73**, 915–924 (1985).
25. Thomas, S. C. in *Size- and Age-Related Changes in Tree Structure and Function* (eds Meinzer, F. C., Lachenbruch, B. & Dawson, T. E.) Ch. 2 33–64 (Springer, 2011).
26. Bigler, C. & Veblen, T. T. Increased early growth rates decrease longevities of conifers in subalpine forests. *Oikos* **118**, 1130–1138 (2009).
27. Di Filippo, A., Biondi, F., Maugeri, M., Schirone, B. & Piovesan, G. Bioclimate and growth history affect beech lifespan in the Italian Alps and Apennines. *Glob. Change Biol.* **18**, 960–972 (2012).
28. LaDeau, S. L. & Clark, J. S. Rising CO2 levels and the fecundity of forest trees. *Science* **292**, 95–98 (2001).
29. Manusch, C., Bugmann, H., Heiri, C. & Wolf, A. Tree mortality in dynamic vegetation models – a key feature for accurately simulating forest properties. *Ecol. Modell.* **243**, 101–111 (2012).
30. Saleska, S. R. *et al.* Carbon in Amazon forests: unexpected seasonal fluxes and disturbance-induced losses. *Science* **302**, 1554–1557 (2003).

R. J. W. Brienen[1]*, O. L. Phillips[1]*, T. R. Feldpausch[1,2], E. Gloor[1], T. R. Baker[1], J. Lloyd[3,4], G. Lopez-Gonzalez[1], A. Monteagudo-Mendoza[5], Y. Malhi[6], S. L. Lewis[1,7], R. Vásquez Martinez[5], M. Alexiades[8], E. Álvarez Dávila[9], P. Alvarez-Loayza[10], A. Andrade[11], L. E. O. C. Aragão[2,12], A. Araujo-Murakami[13], E. J. M. M. Arets[14], L. Arroyo[13], G. A. Aymard C.[15], O. S. Bánki[16], C. Baraloto[17,18], J. Barroso[19], D. Bonal[20], R. G. A. Boot[21], J. L. C. Camargo[11], C. V. Castilho[22], V. Chama[23], K. J. Chao[1,24], J. Chave[25], J. A. Comiskey[26], F. Cornejo Valverde[27], L. da Costa[28], E. A. de Oliveira[29], A. Di Fiore[30], T. L. Erwin[31], S. Fauset[1], M. Forsthofer[29], D. R. Galbraith[1], E. S. Grahame[1], N. Groot[1], B. Hérault[32], N. Higuchi[11], E. N. Honorio Coronado[1,33], H. Keeling[1], T. J. Killeen[34], W. F. Laurance[35], S. Laurance[35], J. Licona[36], W. E. Magnussen[37], B. S. Marimon[29], B. H. Marimon-Junior[29], C. Mendoza[38,39], D. A. Neill[40], E. M. Nogueira[41], P. Núñez[23], N. C. Pallqui Camacho[23], A. Parada[13], G. Pardo-Molina[42], J. Peacock[1], M. Peña-Claros[36,43], G. C. Pickavance[1], N. C. A. Pitman[10,44], L. Poorter[43], A. Prieto[45], C. A. Quesada[41], F. Ramírez[45], H. Ramírez-Angulo[46], Z. Restrepo[9], A. Roopsind[47], A. Rudas[48], R. P. Salomão[49], M. Schwarz[1], N. Silva[50], J. E. Silva-Espejo[23], M. Silveira[51], J. Stropp[52], J. Talbot[1], H. ter Steege[53,54], J. Teran-Aguilar[55], J. Terborgh[10], R. Thomas-Caesar[50], M. Toledo[36], M. Torello-Raventos[56,57], R. K. Umetsu[29], G. M. F. van der Heijden[58,59,60], P. van der Hout[61], I. C. Guimarães Vieira[49], S. A. Vieira[62], E. Vilanova[46], V. A. Vos[42,63] & R. J. Zagt[21]

[1]School of Geography, University of Leeds, Leeds LS2 9JT, UK. [2]Geography, College of Life and Environmental Sciences, University of Exeter, Rennes Drive, Exeter EX4 4RJ, UK. [3]Department of Life Sciences, Imperial College London, Silwood Park Campus, Buckhurst Road, Ascot, Berkshire SL5 7PY, UK. [4]School of Marine and Tropical Biology, James Cook University, Cairns, 4870 Queenland, Australia. [5]Jardín Botánico de Missouri, Prolongacion Bolognesi Mz.e, Lote 6, Oxapampa, Pasco, Peru. [6]Environmental Change Institute, School of Geography and the Environment, University of Oxford, Oxford OX1 3QK, UK. [7]Department of Geography, University College London, Pearson Building, Gower Street, London WC1E 6BT, UK. [8]School of Anthropology and Conservation, Marlowe Building, University of Kent, Canterbury CT1 3EH, UK. [9]Servicios Ecosistemicos y Cambio Climático, Jardín Botánico de Medellín, Calle 73 no. 51 D-14, C.P. 050010, Medellín, Colombia. [10]Center for Tropical Conservation, Duke University, Box 90381, Durham, North Carolina 27708, USA. [11]Biological Dynamics of Forest Fragment Project (INPA & STRI), C.P. 478, Manaus AM 69011-970, Brazil. [12]National Institute for Space Research (INPE), Av. Dos Astronautas, 1758, São José dos Campos, São Paulo 12227-010, Brazil. [13]Museo de Historia Natural Noel Kempff Mercado, Universidad Autonoma Gabriel Rene Moreno, Casilla 2489, Av. Irala 565, Santa Cruz, Bolivia. [14]Alterra, Wageningen University and Research Centre, PO Box 47, 6700 AA Wageningen, The Netherlands. [15]UNELLEZ-Guanare, Programa de Ciencias del Agro y el Mar, Herbario Universitario

(PORT), Mesa de Cavacas, Estado Portuguesa, 3350 Venezuela. [16]Biodiversiteit en Ecosysteem Dynamica, University of Amsterdam, Postbus 94248, 1090 GE Amsterdam, The Netherlands. [17]Institut National de la Recherche Agronomique, UMR EcoFoG, Campus Agronomique, 97310 Kourou, French Guiana. [18]International Center for Tropical Botany, Department of Biological Sciences, Florida International University, Miami, Florida 33199, USA. [19]Universidade Federal do Acre, Campus de Cruzeiro do Sul, Rio Branco, Brazil. [20]INRA, UMR 1137 ''Ecologie et Ecophysiologie Forestiere'' 54280 Champenoux, France. [21]Tropenbos International, PO Box 232, 6700 AE Wageningen, The Netherlands. [22]Embrapa Roraima, Caixa Postal 133, Boa Vista, RR, CEP 69301-970, Brazil. [23]Universidad Nacional San Antonio Abad del Cusco, Av. de la Cultura N° 733, Cusco, Peru. [24]International Master Program of Agriculture, College of Agriculture and Natural Resources, National Chung Hsing University, Taichung 40227, Taiwan. [25]Université Paul Sabatier CNRS, UMR 5174 Evolution et Diversité Biologique, Bâtiment 4R1, 31062 Toulouse, France. [26]Northeast Region Inventory and Monitoring Program, National Park Service, 120 Chatham Lane, Fredericksburg, Virginia 22405, USA. [27]Andes to Amazon Biodiversity Program, Puerto Maldonado, Madre de Dios, Peru. [28]Universidade Federal do Para, Centro de Geociencias, Belem, CEP 66017-970 Para, Brazil. [29]Universidade do Estado de Mato Grosso, Campus de Nova Xavantina, Caixa Postal 08, CEP 78.690-000, Nova Xavantina MT, Brazil. [30]Department of Anthropology, University of Texas at Austin, SAC Room 5.150, 2201 Speedway Stop C3200, Austin, Texas 78712, USA. [31]Department of Entomology, Smithsonian Institution, PO Box 37012, MRC 187, Washington DC 20013-7012, USA. [32]Cirad, UMR Ecologie des Forêts de Guyane, Campus Agronomique, 97310 Kourou, French Guiana. [33]Instituto de Investigaciones de la Amazonía Peruana, Av. A. José Quiñones km 2.5, Iquitos, Peru. [34]World Wildlife Fund, 1250 24th Street NW, Washington DC 20037, USA. [35]Centre for Tropical Environmental and Sustainability Science (TESS) and School of Marine and Environmental Sciences, James Cook University, Cairns, Queensland 4878, Australia. [36]Instituto Boliviano de Investigación Forestal, C.P. 6201, Santa Cruz de la Sierra, Bolivia. [37]National Institute for Research in Amazonia (INPA), C.P. 478, Manaus, Amazonas, CEP 69011-970, Brazil. [38]FOMABO, Manejo Forestal en las Tierras Tropicales de Bolivia, Sacta, Bolivia. [39]Escuela de Ciencias Forestales (ESFOR), Universidad Mayor de San Simón (UMSS), Sacta, Bolivia. [40]Universidad Estatal Amazónica, Facultad de Ingeniería Ambiental, Paso lateral km 2 1/2 via Napo, Puyo, Pastaza, Ecuador. [41]National Institute for Research in Amazonia (INPA), C.P. 2223, 69080-971, Manaus, Amazonas, Brazil. [42]Universidad Autonoma del Beni, Campus Universitario, Av. Ejército Nacional, Riberalta, Beni, Bolivia. [43]Forest Ecology and Forest Management Group, Wageningen University, PO Box 47, 6700 AA Wageningen, The Netherlands. [44]The Field Museum, 1400 South Lake Shore Drive, Chicago, Illinois 60605-2496, USA. [45]Universidad Nacional de la Amazonía Peruana, Iquitos, Loreto, Peru. [46]Instituto de Investigaciones para el Desarrollo Forestal (INDEFOR), Universidad de Los Andes, Facultad de Ciencias Forestales y Ambientales, Conjunto Forestal, C.P. 5101, Mérida, Venezuela. [47]Iwokrama International Centre for Rainforest Conservation and Development, 77 High Street Kingston, Georgetown, Guyana. [48]Instituto de Ciencias Naturales, Universidad Nacional de Colombia, Ciudad Universitaria, Carrera 30 No 45-03, Edificio 425, C.P. 111321, Bogota, Colombia. [49]Museu Paraense Emilio Goeldi, Av. Magalhães Barata, 376 - São Braz, CEP 66040-170, Belém PA, Brazil. [50]UFRA, Av. Presidente Tancredo Neves 2501, CEP 66.077-901, Belém, Pará, Brazil. [51]Museu Universitário, Universidade Federal do Acre, Rio Branco AC 69910-900, Brazil. [52]European Commission – DG Joint Research Centre, Institute for Environment and Sustainability, Via Enrico Fermi 274, 21010 Ispra, Italy. [53]Naturalis Biodiversity Center, PO Box, 2300 RA, Leiden, The Netherlands. [54]Ecology and Biodiversity Group, Utrecht University, PO Box 80084, 3508 TB Utrecht, The Netherlands. [55]Museo de Historia Natural Alcide D'Orbigny, Av. Potosi no 1458, Cochabamba, Bolivia. [56]School of Earth and Environmental Science, James Cook University, Cairns, Queensland 4870, Australia. [57]Centre for Tropical Environmental and Sustainability Science (TESS) and School of Marine and Tropical Biology, James Cook University, Cairns, Queensland 4878, Australia. [58]Northumbria University, School of Geography, Ellison Place, Newcastle upon Tyne, Newcastle NE1 8ST, UK. [59]University of Wisconsin, Milwaukee, Wisconsin 53202, USA. [60]Smithsonian Tropical Research Institute, Apartado Postal 0843-03092, Panamá, Republic of Panama. [61]Van der Hout Forestry Consulting, Jan Trooststraat 6, 3078 HP Rotterdam, The Netherlands. [62]Universidade Estadual de Campinas, NEPAM, Rua dos Flamboyants, 155- Cidade Universitária Zeferino Vaz, Campinas, CEP 13083-867, Sao Paulo, Brazil. [63]Centro de Investigación y Promoción del Campesinado, regional Norte Amazónico, C/ Nicanor Gonzalo Salvatierra N° 362, Casilla 16, Riberalta, Bolivia.

*These authors contributed equally to this work.

METHODS

Forest biometric data. Mature forests were sampled throughout the forested lowland tropical areas of South America (below 1,500 m above sea level) that receive at least 1,000 mm of rainfall annually. To be included in this study, permanent sample plots were required to have two or more censuses. Immature or open forests, and those known to have had anthropogenic disturbances owing to fire or selective logging, were excluded. The plots are geographically well dispersed throughout the Amazon Basin (Extended Data Fig. 1), covering every tropical South American country except Suriname. Supplementary Table 1 includes a complete list of plots included in this study with the respective size, start and end date for the censuses included in this analysis, and names of the main researchers for each plot. A full manual for plot establishment and tree measurements of the RAINFOR plot network can be found in ref. 31.

Of the total 321 plots, 232 are from the RAINFOR network. In addition, we compiled biomass dynamics data for 89 plots from published studies, mostly from one site for 2001 to 2003 (DUK) (see Supplementary Table 1). For these plots, we simply used the available biomass data as published. Note that these studies do not apply the same allometric equations, and may have slightly different measurements protocols and census interval corrections. While as a general rule all trees with stem diameters greater than 100 mm were included in this analysis, palms (Arecaceae) or coarse herbs of the genus *Phenakospermum* were excluded for a few plots (19) due to changes in measurement protocols over time in these plots. In addition, for a few plots only trees $\geq$130 or $\geq$200 mm in diameter were recorded in the first census(es). In these cases, we either standardized the biomass data in the first census(es) to trees $\geq$100 mm using the ratio of biomass for trees $\geq$100 and $\geq$200 mm (seven plots) of later censuses, or we used the slightly different minimum size threshold for the full period, including only trees $\geq$130 mm (for two plots). For full details on these specific issues see the online source data. For analysis purposes, plots smaller than 0.5 ha that were within 1 km or less of one another were merged, to give a total of 274 'sample units'. The mean size across all sample units was 1.24 ha, and the mean total monitoring period was 11.1 years. In total, the study monitored 343 ha for a combined total of 4,620 ha years, involving more than 850,000 tree measurements on around 189,000 individual trees larger than 10 cm diameter.

The standard protocol for tree measurements in the field is to measure diameter at breast height, defined as 1.3 m from the base of the stem. For non-cylindrical stems owing to buttresses or other deformities the point of measurement is raised approximately 50 cm above the deformity. The exact height of the point of measurement (POM) was recorded and marked on the trees to ensure that future measurements were taken at the same point. For those trees where buttress growth threatened to reach the initial POM, we raised the height of diameter measurement to a new POM, located sufficiently high above the buttresses to avoid interference of buttresses with diameter measurements at subsequent censuses. If a change in POM was made, we recorded both the diameter at the original POM and the new POM, thus creating two disjoint series of diameters measured at different heights. To avoid potential biases that can result from not accounting for the POM movement, following ref. 32 we computed a new diameter series that was calculated as the mean of: (1) diameter measurements standardized to the new (final) POM, obtained by multiplication of measurements at the original POM by the ratio between diameter measurements at the new and original POM, and (2) diameter measurements standardized to the original POM, by multiplying measurements at the new POM by the ratio between diameter measurements at the original and new POM. The outcome of our analysis was robust with respect to the method of dealing with POM changes, giving similar results using several alternative approaches for dealing with POM changes including the technique described previously[17] in which diameter gains at the new POM are added to the diameter at the original POM. Following ref. 32 we used several techniques to avoid or minimise potential errors arising from missing diameter values, typographical errors, or extreme diameter growth $\geq$4 cm yr^{-1} or total diameter growth $\leq$$-$0.5 cm across a single census interval (that is, losing 0.5 cm, as trees may shrink by a small amount due to hydrostatic effects in times of drought, and measurement errors can be both positive and negative). For stems belonging to species known to experience very high growth rates or noted as having damaged stems we accepted these values. We used interpolation, where possible, else extrapolation to correct errors. If neither of these procedures were possible we used the mean growth rate of all dicotyledonous stems in the same plot census, belonging to the same size class, with size classes defined as 10 $\leq$ diameter < 20 cm, 20 $\leq$ diameter < 40 cm, and diameter $\geq$ 40 cm, to estimate the missing diameter value. Of all stem growth increments, for 1.7% per census we assigned interpolated estimates of diameter, for 0.9% we used extrapolated estimates, and for 1.5% we used mean growth rates.

Computing above ground biomass, sampling effects and scaling up sink estimates. We converted diameter measurements to AGB estimates using allometric equations described previously[8], which include terms for wood density, diameter and tree height. Tree height was estimated based on established diameter-height

relations that vary between the different regions of Amazonia[8]. Wood density values were extracted from a global wood density database (http://datadryad.org/handle/10255/dryad.235; ref. 33). In cases where a stem was unidentified or where no taxon-specific wood density data were available, we applied the appropriate genus or family-specific wood density values. If none of those was available, the mean wood density of all identified dicotyledenous tree stems in the plot was applied. In our analysis 80% of the trees were identified to species level, 94% to genus level, and 97% to family level. All data on tree diameter, taxonomy, and associated botanical vouchers are curated under the https://www.forestplots.net/ web application and database[34].

The magnitude of the biomass sink for the forested area of the Amazon Basin for the 1990s and 2000s was estimated by multiplying the magnitude of total biomass change with an estimated area of intact forest, including all open and closed, evergreen and deciduous forests for tropical South America (6.29 × 10^8 ha, according to Global Land Cover map 2000; ref. 35). For this calculation we also included biomass components that were not directly measured, assuming that these pools responded proportionally to the measured above ground biomass in trees bigger than 10 cm in diameter. It has been shown using destructive measurements of stand biomass in central Amazonia that lianas and trees smaller than 100 mm in diameter represent an additional fraction of ~9.9% the measured AGB (in trees $\geq$10 cm in diameter[36]), and below ground biomass a fraction of ~37% the AGB[36]. We assumed that 50% of biomass is carbon[37].

Analysing time trends and statistical analysis. The longer a census interval, the greater the proportion of growth that cannot be directly observed within the interval, due to the growth of initially recorded trees that subsequently die during the interval, and the growth of unrecorded trees that both recruit and die during the interval[38–40]. Hence, variation in census interval lengths in plots over time will affect estimates of woody productivity and mortality rates[40], potentially biasing the long-term trends if not accounted for. Using established procedures[32], we therefore explicitly corrected for the influence of varying census interval length, by estimating the following two unobserved components: (1) unobserved recruits, that is, the cohort of recruits that both enter and die between two successive censuses, and (2) unobserved biomass growth and mortality, due to the growth of trees after the final census that a tree was recorded alive. To correct for unobserved recruits, we first estimated the number of unobserved recruits (U_r) as the number of stems in the plot (N) multiplied by the annual recruitment rate (R) multiplied by the mean annual mortality rate (M) multiplied by the census interval length (t): $U_r = N \times R \times M \times t$. We assumed that the diameter of these trees was 100 mm plus growth for one-third of the interval using the median growth rate for trees in the 100–200 mm size class. The biomass of each tree was estimated by applying the regionally appropriate allometric equation[8], using the plot mean wood density. To correct for unobserved growth and mortality due to trees dying within an interval, we assumed that all trees that died during the interval to have died at the mid-point, and assigned growth up to this mid-point, estimated as the median growth of all trees in the plot within the same size class. Full details of the procedure have been described previously[32]. These estimates of the unobserved biomass dynamics usually accounted for only a small proportion of the total woody productivity and mortality (respectively 2.28% and 2.74%, on average).

Mean time trends of biomass dynamics (black lines in Fig. 1 and Extended Data Figs 3 and 5–7) were calculated for each month since 1983 as the weighted mean across all sample units. As plots vary in total area monitored, we used an empirical weighting procedure to account for differences between plots in sampling effort by weighting according to the square root of plot area[4,41]. Confidence intervals (95%) were estimated using weighted bootstrap sampling.

To estimate long-term trends in biomass dynamics (cf. Figure 1), we first used general additive mixed models (GAMM) from the gamm4 R package[42]. Estimates of the long-term trends were performed by regressing the mid-point of each census interval (Extended Data Fig. 2) against the rate of change (net change, mortality or gains). Here, systematic plot effects were explicitly accounted for by using plot as a random effect in the model. This avoided switches over time in the exact set of plots being monitored influencing the long-term trends. As census interval length and plot sizes varied, we weighted each data point in the regression by the product of the census interval length (in years) times the square root of plot size (in hectares), as suggested previously[41]. We estimated the linear slope of the long-term trend using the lme4 package[43]. In an identical way to the GAMM, we accounted for plot effects and added weights to the regression. To test whether the estimated time trends were robust to different plots being sampled over different timeframes, we also repeated the above analysis over shorter time windows (1990–2011.5, 1995–2011.5 and 2000–2011.5) keeping the set of plots used completely constant. Results of this analysis are shown in Extended Data Fig. 3.

The approaches using GAMM and the linear slope calculations are parametric and assume normally distributed data, while census-level data on AGB mortality and net AGB change are non-normally distributed, showing respectively right-skewed

and left-skewed distributions. Thus the observed time series for AGB mortality and net AGB change do not strictly meet the criteria for this type of parametric analysis, although it might be expected from the central limit theorem that with sufficiently large data sets the regression analyses would still have validity. To test explicitly the robustness of our estimates for the models of net change and mortality with regard to violation of the normality assumption for ordinary least squares analysis, we used a rank-based estimator for linear models available from the Rfit-package[44]. This shows that slopes for AGB net change and mortality are similar or else of larger magnitude using non-parametric tests (that is, slope net change = -0.057 Mg ha^{-1} yr^{-2}, $P < 0.001$, slope mortality = 0.061 Mg ha^{-1} yr^{-2}, $P < 0.001$, compared respectively to values of -0.034 Mg ha^{-1} yr^{-2} and 0.051 Mg ha^{-1} yr^{-2} using the parametric techniques). A test of non-parametric rank based estimations of the slopes of the change in standing biomass, or mortality on a per stem basis (Extended Data Fig. 6), and of changes in stem numbers and number of trees dying and recruiting per hectare (Extended Data Fig. 7), or basal area changes (Extended Data Fig. 8), show similar results to that of the parametric tests: there is a significant decrease in net change of standing biomass per stem ($P = 0.0014$), no trend in the losses on a per-stem basis ($P = 0.47$), a significant decrease in the change in the number of stems per hectare ($P < 0.001$), marginally significant increase in number of recruits ($P = 0.051$), a significant increase in the number of trees dying ($P < 0.001$), a significant decrease in net basal area change ($P < 0.001$), and a significant increase in basal area mortality ($P < 0.001$).

A second method for calculating the long-term trends in biomass dynamics involved estimating the slopes of the time trends for individual plots (Fig. 2). We did this only for those plots that had at least three census intervals, and more than 10 years of total monitoring length with at least one census interval in the 1990s and in the 2000s. These stricter selection criteria were designed to allow us to focus on a core set of data most likely to capture long-term patterns in regional biomass dynamics. Slopes of biomass dynamics metrics were seldom statistically significant ($P = 0.95$) within plots, due to the stochastic nature of the dynamics data (Extended Data Fig. 2). We calculated the mean of the slopes across all plots weighted by the product of square root of plot area times the total census interval length. A t-test was used to test whether the mean values were significantly different from zero.

All analyses was performed using the R statistical platform, version 3.0.2 (ref. 45). No statistical methods were used to predetermine sample size.

31. Phillips, O., Baker, T., Brienen, R. & Feldpausch, T. RAINFOR field manual for plot establishment and remeasurement. http://www.rainfor.org/upload/ManualsEnglish/RAINFOR_field_manual_version_June_2009_ENG.pdf (2010).
32. Talbot, J. et al. Methods to estimate aboveground wood productivity from long-term forest inventory plots. For. Ecol. Management 320, 30–38 (2014).
33. Chave, J. et al. Towards a worldwide wood economics spectrum. Ecol. Lett. 12, 351–366 (2009).
34. Lopez-Gonzalez, G., Lewis, S. L., Burkitt, M. & Phillips, O. L. ForestPlots.net: a web application and research tool to manage and analyse tropical forest plot data. J. Veg. Sci. 22, 610–613 (2011).
35. Bartholomé, E. & Belward, A. GLC2000: a new approach to global land cover mapping from Earth observation data. Int. J. Remote Sens. 26, 1959–1977 (2005).
36. Phillips, O. L., Lewis, S. L., Baker, T. R., Chao, K. J. & Higuchi, N. The changing Amazon forest. Phil. Trans. R. Soc. Lond. B 363, 1819–1827 (2008).
37. Chave, J. et al. Tree allometry and improved estimation of carbon stocks and balance in tropical forests. Oecologia 145, 87–99 (2005).
38. Sheil, D. & May, R. M. Mortality and recruitment rate evaluations in heterogeneous tropical forests. J. Ecol. 84, 91–100 (1996).
39. Malhi, Y. et al. The above-ground coarse wood productivity of 104 Neotropical forest plots. Glob. Change Biol. 10, 563–591 (2004).
40. Lewis, S. L. et al. Tropical forest tree mortality, recruitment and turnover rates: calculation, interpretation and comparison when census intervals vary. J. Ecol. 92, 929–944 (2004).
41. Muller-Landau, H. C., Detto, M., Chisholm, R. A., Hubbell, S. P. & Condit, R. in Forests and Global Change ecological reviews (eds Coomes, D., Burslem, D. F. R. P. & Simonson, W. D.) Ch. 14 462 (Cambridge Univ. Press, 2014).
42. Wood, S. gamm4: Generalized additive mixed models using mgcv and lme4. R package version 0.1–2. Available at http://www.inside-r.org/packages/gamm4/versions/0-1-2 (2011).
43. Bates, D., Maechler, M., Bolker, B. & Walker, S. lme4: Linear mixed-effects models using Eigen and S4. R package version, 1.0-4. Available at http://www.inside-r.org/packages/lme4/versions/1-0-4 (2013).
44. Kloke, J. D. & McKean, J. W. Rfit: Rank-based estimation for linear models. Rem. J. 4, 57–64 (2012).
45. R. Development Core Team. R: A Language and Environment for Statistical Computing. Available at http://www.R-project.org/ (2013).
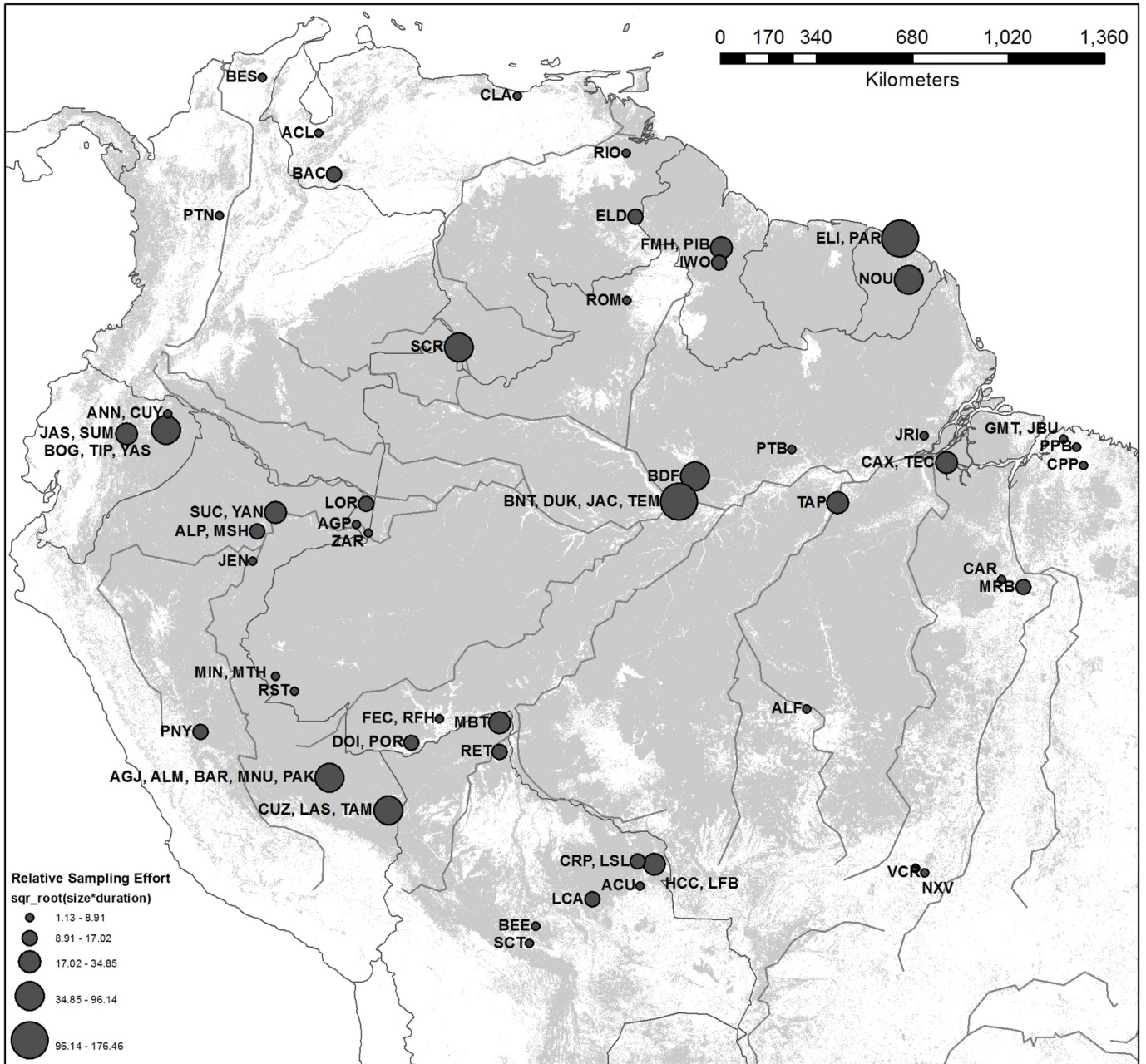
Extended Data Figure 1 | Map showing locations of plots included in this study. The three-letter codes refer to plot codes (see Supplementary Table 1). Adjacent plots (<50 km apart) are shown as one for display purposes. Size of the dots corresponds to the relative sampling effort at that location which is calculated as the square root of plot size multiplied by square root of census length. The grey area shows the cover of all open and closed, evergreen and deciduous forests for tropical South America, according to Global Land Cover map 2000 (ref. 35).
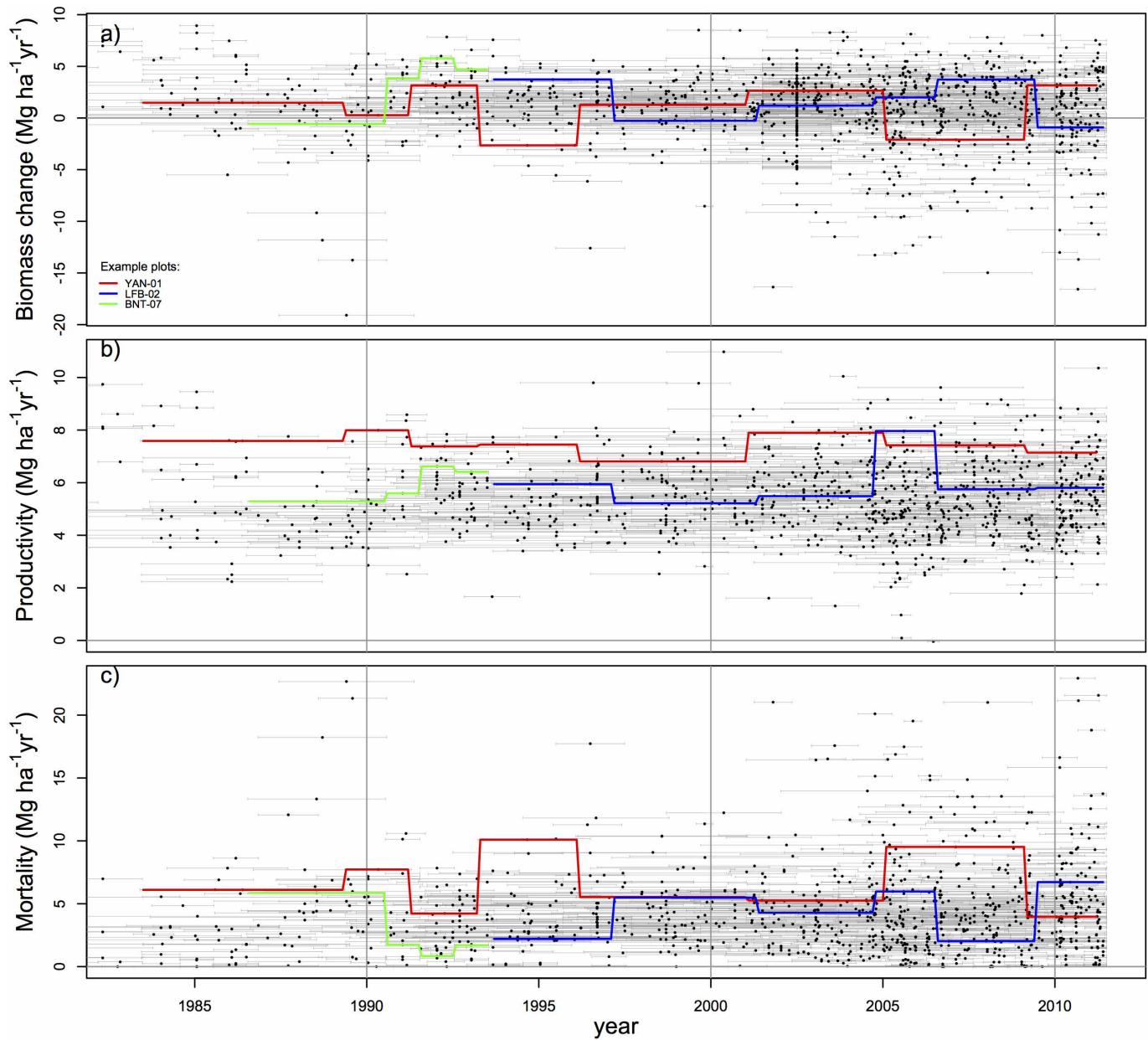
Extended Data Figure 2 | Scatterplot of mid-interval date against net AGB change, AGB productivity and AGB loss due to mortality for all data points and plots used in this analysis. **a**, Biomass change. **b**, Productivity. **c**, Mortality. Points indicate the mid-census interval date, while horizontal error-bars connect the start and end date for each census interval. To illustrate variation in net AGB change over time within individual plots, examples of time series for three individual plots are show as lines.
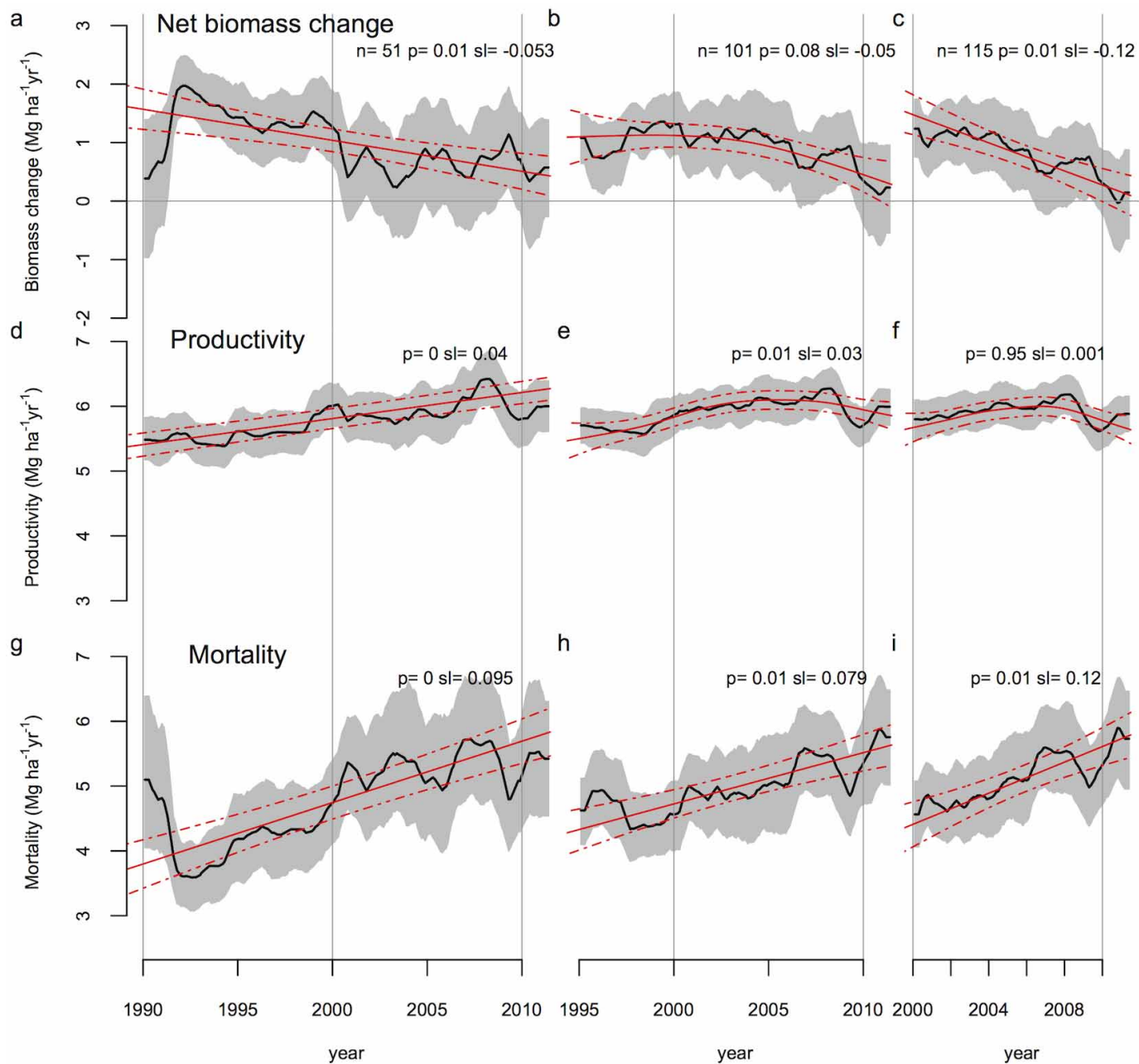
Extended Data Figure 3 | Time trends of subsets of net above-ground biomass change, above-ground woody productivity and mortality rates for plots that were continuously monitored throughout, for the periods 1990–2011, 1995–2011 and 2000–2011. Locations for the set of plots included in the analysis for the different periods are show in the maps in lower panels. The red lines indicate the best model fit for the long-term trends using General Additive Mixed Models (GAMM) accounting explicitly for differences in dynamics between plots (red lines denote overall mean, broken lines denote s.e.m.). Estimated long-term (linear) mean slopes (sl), P values and sample sizes (n) are indicated (see Methods).
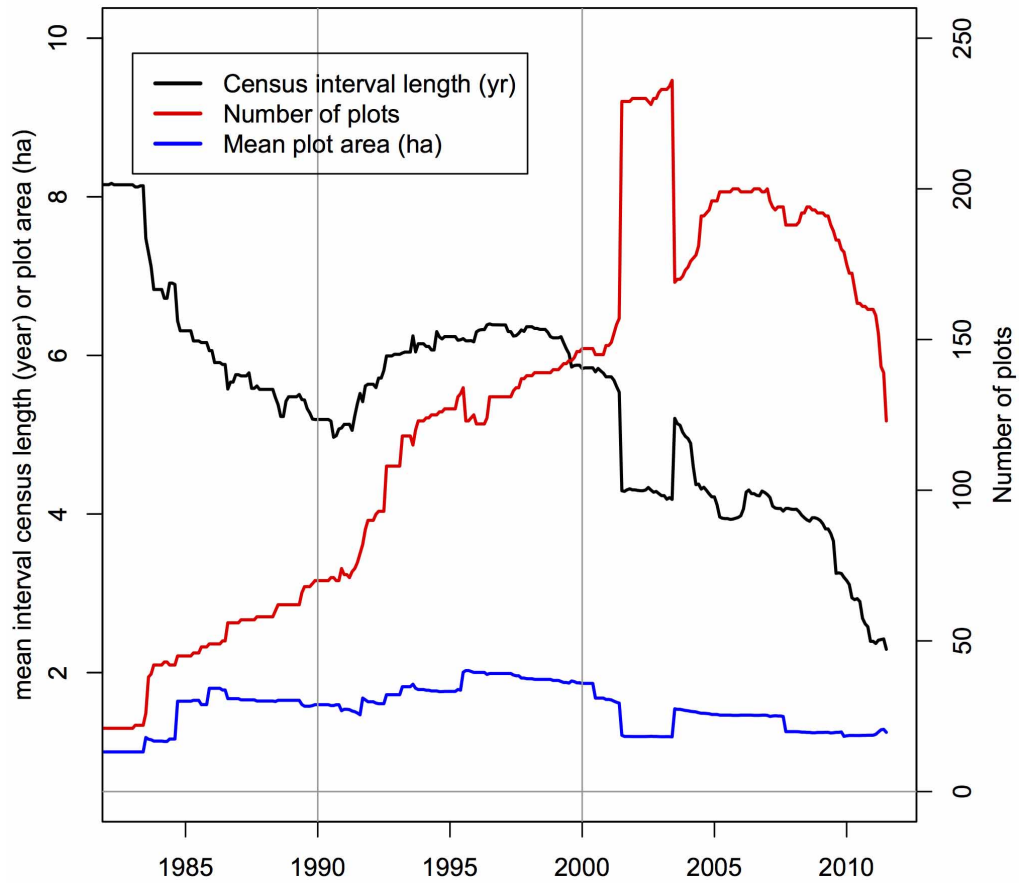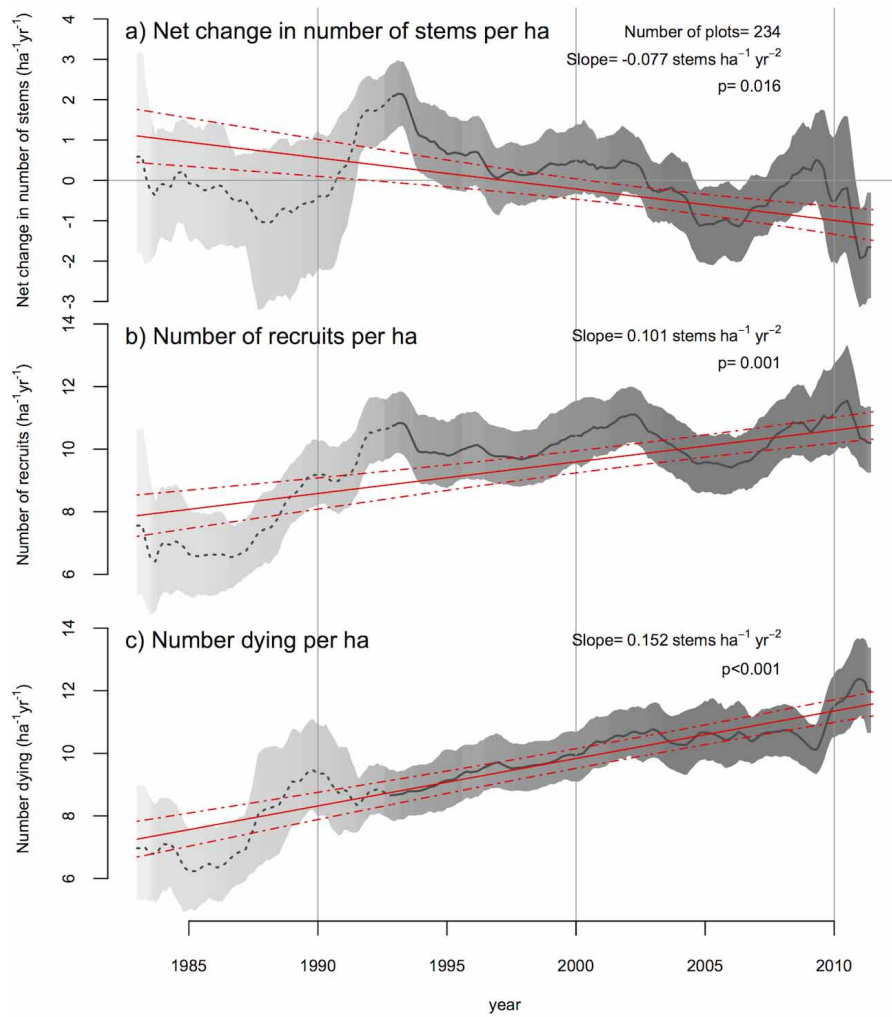
Extended Data Figure 4 | Mean number of plots, interval census length and area of all plots. The mean number of plots (red lines), mean interval census length (black lines) and mean plot area (blue lines) are shown. Note that the increased sampling in 2002 to 2004 is largely due to the short-term addition of 72 plots from one site (Ducke, north of Manaus), but this has no discernible effect on averaged biomass dynamics (Fig. 1).
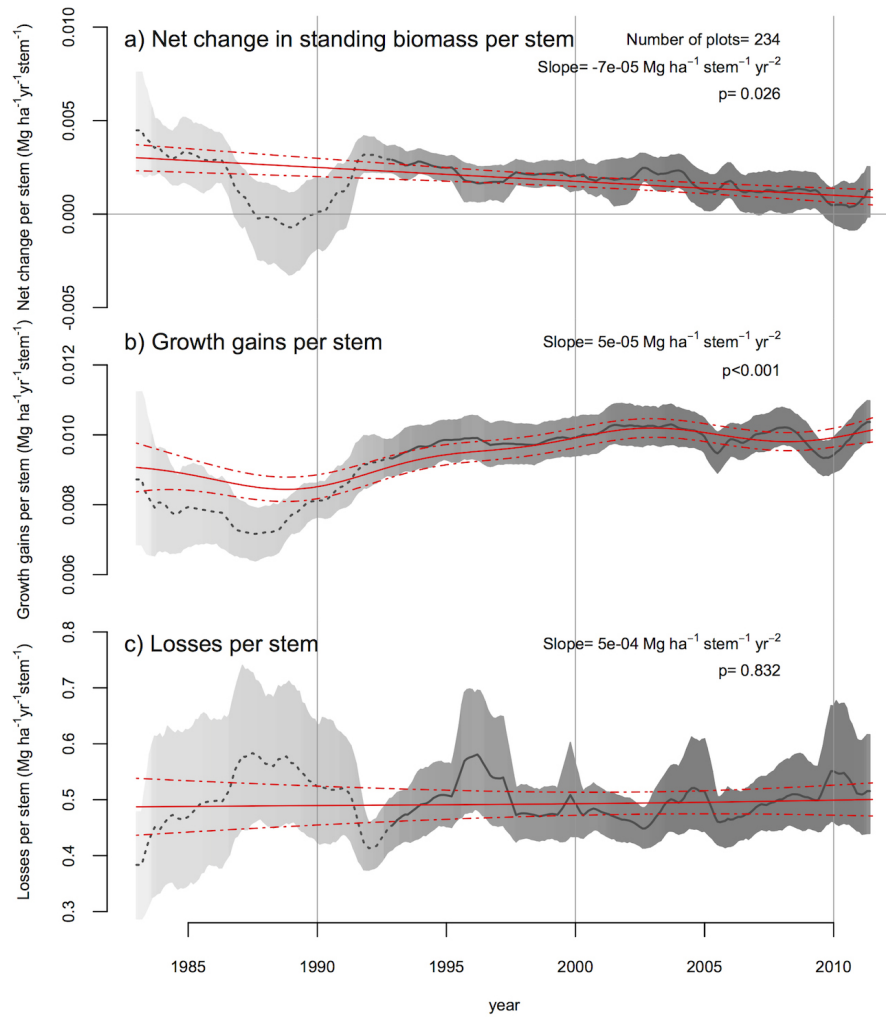
Extended Data Figure 5 | Biomass change, growth gains and mortalities on a per live stem basis. a, Mean net biomass change on a per live stem basis (that is, net biomass change per stem). **b**, Mean growth gains per live tree (that is, mean biomass accumulation of individual trees). **c**, Mortality losses per stem. Analyses are based on 234 plots, excluding published studies without available stem-by-stem data. The red lines indicate the best model fit for the long-term trends using General Additive Mixed Models (GAMM) accounting explicitly for differences in dynamics between plots (red lines denote overall mean, broken lines denote s.e.m.). Estimated long-term (linear) mean slopes and significance levels are indicated (see Methods).

Extended Data Figure 6 | Rates of change in number of stems plus annualized fluxes of stems bigger than 10 cm in diameter. a–c, Mean net change in number of stems (**a**), number of recruits (**b**), and and number of dying trees (**c**). Analyses are based on 234 plots, excluding published studies without available stem-by-stem data. The red lines indicate the best model fit for the long-term trends using General Additive Mixed Models (GAMM) accounting explicitly for differences in dynamics between plots (red lines denote overall mean, broken lines denote s.e.m.). Estimated long-term (linear) mean slopes and significance levels are indicated (see Methods).
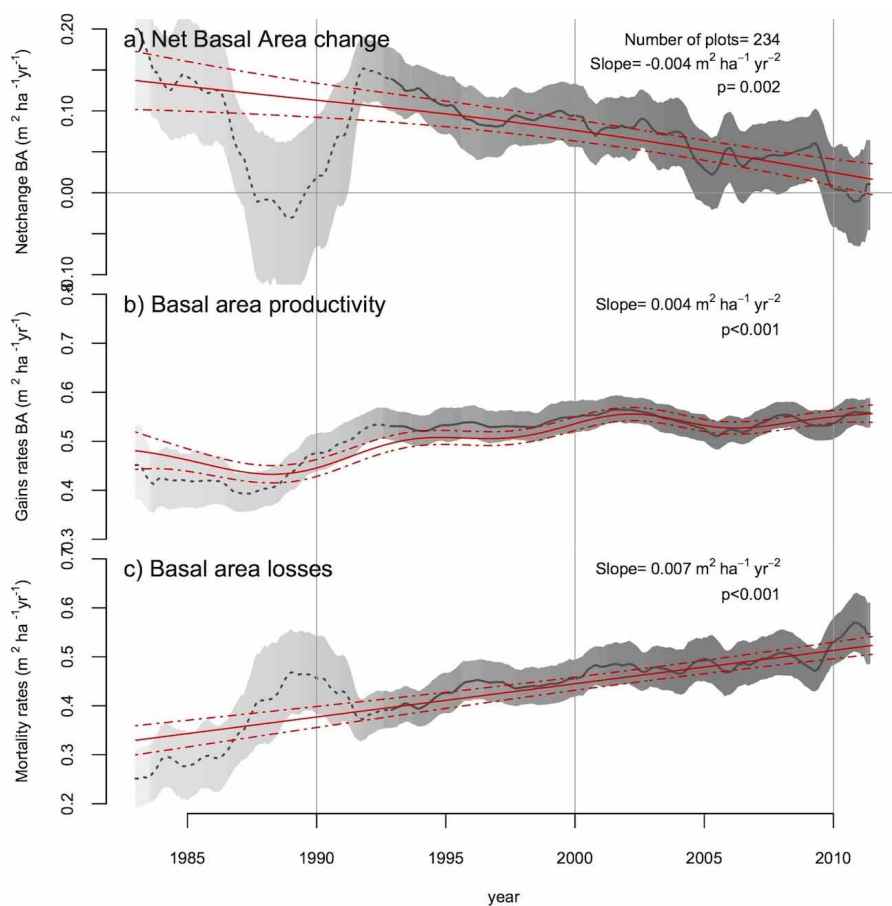
Extended Data Figure 7 | Basal area change, productivity and mortality.
a, Mean net basal area change. **b**, Mean basal area productivity. **c**, Mean basal area mortality. Analyses are based on 234 plots, excluding published studies without available basal-area data. The red lines indicate the best model fit for the long-term trends using General Additive Mixed Models (GAMM) accounting explicitly for differences in dynamics between plots (red lines denote overall mean, broken lines denote s.e.m.). Estimated long-term (linear) mean slopes and significance levels are indicated (see Methods).
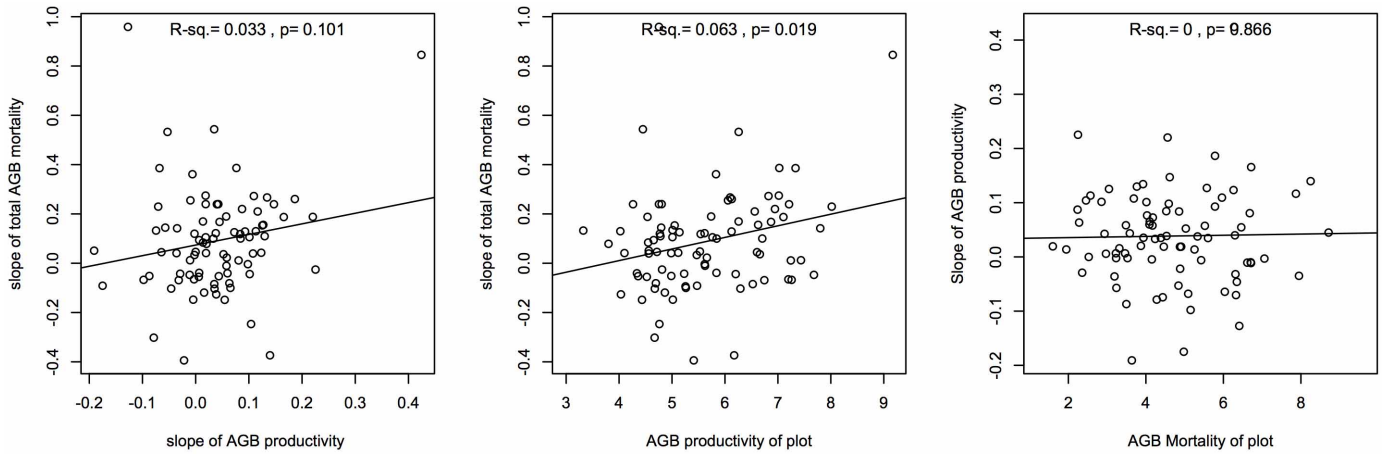
Extended Data Figure 8 | Relationship among plots between mean and slopes of AGB mortality and AGB productivity. a, Scatterplot of the slope of AGB mortality of individual plots against the slope of AGB productivity of plots. **b**, Scatterplot of the slope of AGB loss due to mortality of individual plots against t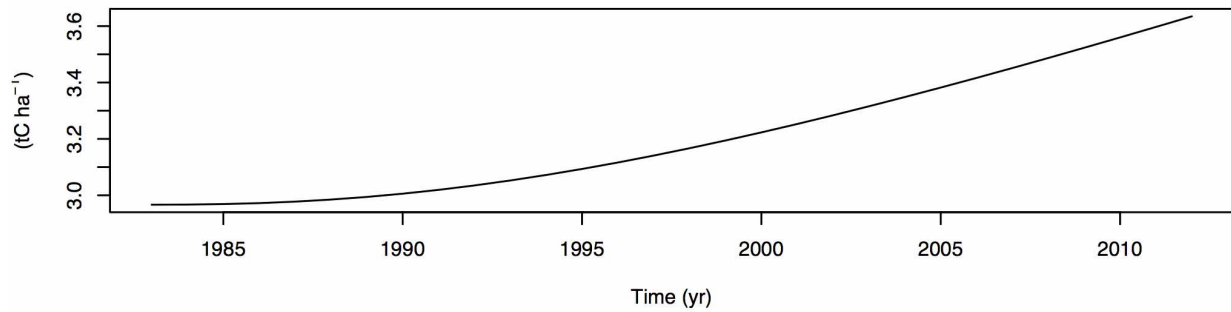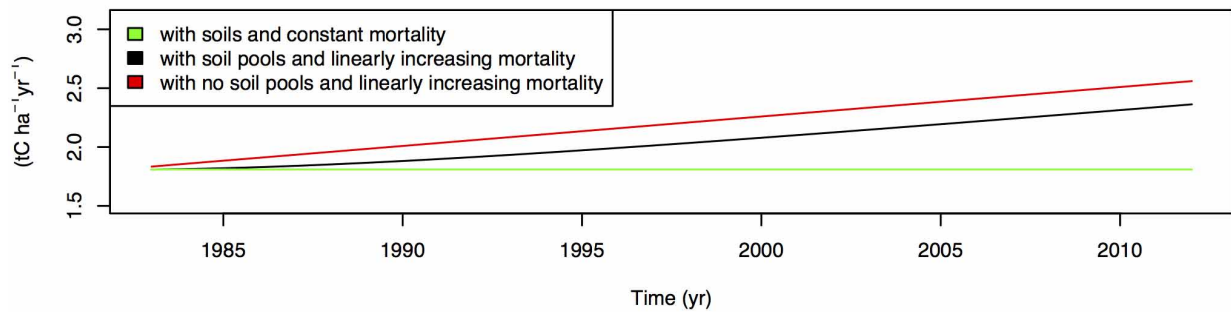he mean AGB productivity of plots. **c**, Scatterplot of the slope of AGB productivity of individual plots against the mean AGB loss due to mortality of plots. The set of plots used in this analysis (117 plots, 87 units) includes only those that had at least 10 years of data and at least three census intervals (that is, same criteria as plots shown in Fig. 2).
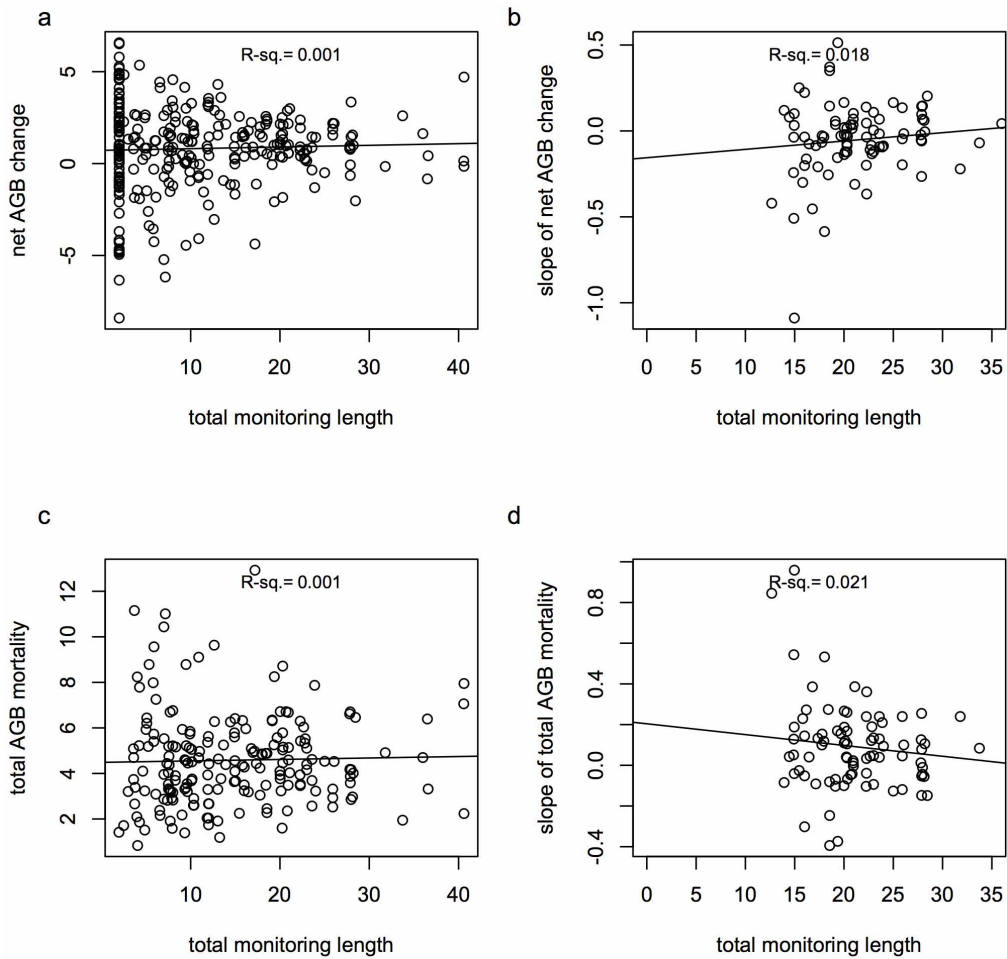
Extended Data Figure 9 | Net AGB change or loss due to mortality versus the total monitoring length of plots, and the slope of net AGB change or mortality versus the total monitoring length of plots. a–d, Scatterplots of net AGB change (**a**) or net AGB loss due to mortality of individual plots (**c**) against the total monitoring length of plots, and the slope of net AGB change (**b**) or slope of AGB mortality of individual plots (**d**) against the total monitoring length of plots. None of the relationships are significant ($P > 0.05$). Note that the plots (117 plots, 87 units) used in **b** and **d** are only those that had at least 10 years of data and at least three census intervals (that is, same criteria as plots shown in Fig. 2). See Supplementary Information for discussion of these results.

a) Necromass for linearly increasing mortality
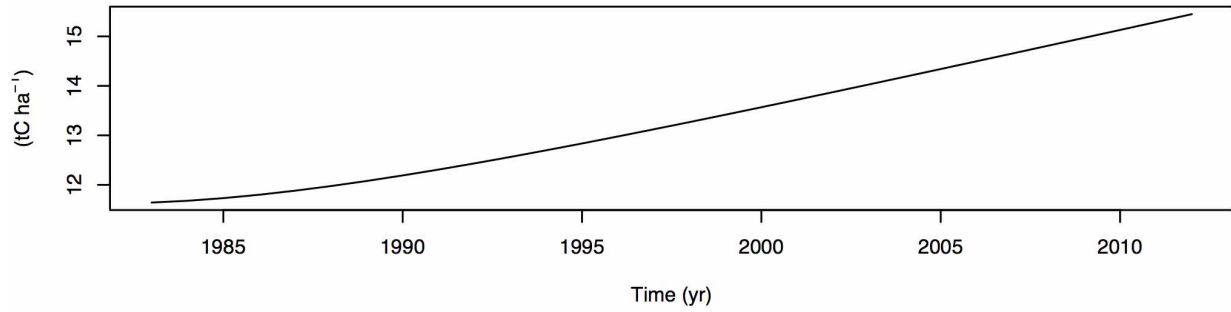
b) Soil organic matter for linearly increasing mortality

c) Flux to atmosphere from necromass

Legend:
- with soils and constant mortality
- with soil pools and linearly increasing mortality
- with no soil pools and linearly increasing mortality

Extended Data Figure 10 | Modelled estimates of the effects of linearly increasing mortality on necromass stocks and soil organic-matter stocks. a, Necromass stocks. **b**, Soil organic matter stocks. **c**, The estimated fluxes of carbon from the forest to the atmosphere in three scenarios: (1) assuming constant mortality rate and a lag in decomposition of dead-tree biomass (green), (2) assuming an increasing mortality rate similar to the observed trend (Fig. 1c) and a lag in decomposition as modelled (black), and (3) with increasing mortality but with all dead-tree biomass instantly respired (red). See Supplementary Information for discussion of these results.